Journal Homepage: http://ijcpe.uobaghdad.edu.iq
Iraqi Journal of Chemical and Petroleum Engineering
Vol. 27 No. 1 (March 2026) 93 – 104
EISSN: 2618-0707, PISSN: 1997-4884

Ciprofloxacin adsorption via compressed wood activated carbon with $ZnCl_2$ activating agent from simulated wastewater: Mechanism studying

Dhuha Hameed Hamad [a, *], Haider A. Al-Jendeel [a], Mustafa Hathal [b]

a Department of Chemical Engineering, College of Engineering, University of Baghdad, Aljadria, Baghdad, 10071, Iraq
b Sustainable Solution Research Lab., University of Pannonia, Veszprem, Hungary

Abstract

The current study objective is to synthesize activated carbon (AC) from compressed wood using the ZnCl2 activating agent and to assess the ciprofloxacin (CIP) elimination efficiency in simulated wastewater. The produced AC was characterized using multiple techniques, including SEM, BET, FTIR, AFM, and XRD. The adsorbent demonstrates high adsorption performance, achieving 91% removal of CIP within 5 hours at an initial pollutant concentration of 100 mg/L with an AC dose of 2 g/L. Experimental data correspond to the Freundlich isotherm model (R^2 = 0.995) as well as the Langmuir competitive fitting (R^2 = 0.99), while the root mean square error (RMSE) equation best fits the Langmuir model. Moreover, the pseudo-second-order model (R^2 = 0.999) was used to describe the kinetic data. The adsorption thermodynamics indicate spontaneous adsorption with exothermic behavior (ΔG°<0, ΔH°<0, ΔS°<0). A combination of mechanisms contributed to the CIP adsorption process (π-π interaction, hydrophobic interaction, bulk diffusion, hydrogen bonds, in addition to physical and chemical adsorption mechanisms). Pyrolysis recoverability shows a good result after three cycles (qe = 101.08 mg/g, compared to 170.13 mg/g in the first cycle). In conclusion, compressed wood AC offers a sustainable, low-cost adsorbent for treating wastewater and presents a prospect for addressing ecosystem contamination challenges.

Keywords: Compressed wood; activated carbon; $ZnCl_2$ activating agent; intraparticle diffusion; Temkin model; ciprofloxacin; adsorption mechanism; exothermic adsorption.

Received on 13/07/2025, Received in Revised Form on 16/08/2025, Accepted on 16/08/2025, Published on 30/03/2026

https://doi.org/10.31699/IJCPE.2026.1.8

1- Introduction

Water reuse is an essential challenge worldwide due to its vital role in human life [1]. Many pollutants that are discharged through water resources include heavy metals, dyes, pesticides, and pharmaceuticals [2]. Therefore, 99% of water around the earth cannot be utilized, as mentioned in (WHO) [3]. Therefore, the ecosystem faces significant threats that affect human health [4]. Among many forms of ecosystem pollution, pharmaceutical contaminants have become a significant challenge for the scientific community, prompting extensive research [5, 6]. These contaminants enter the environment from pharmaceutical industries, consumer excretion, and hospitals [7]. Pharmaceuticals include many categories, such as hormones, steroids, pain relievers, antipyretics, lipid regulators, and antibiotics [8]. Antibiotics are categorized according to the mechanisms of action and chemical structures, for example, sulfonamides, aminosides, tetracyclines, and fluoroquinolones [9].

CIP is one of the most essential fluoroquinolones due to its stability and effectiveness [10] and was developed in 1983 by the German pharmaceutical company Bayer A.G. [11]. CIP is currently used against widely types of bacteria like gram-positive and gram-negative ones compared to limited useful in the early years where restricted at typhoid and legionella bacteria [12], that development microorganisms' resistance to antibiotics due to its difficult biodegradation and the complex characteristics [13] Thus, an effective method should be developed for CIP elimination to protect the environment from this contamination [14].

Activated carbon is one of the favorite adsorbents for its ability to be derived from various precursors, such as banana stalk [15]. Pulp mill sludge and rice straw [16], Coconut shell [17], Sugarcane bagasse [18], Elm tree [19], corncobs [20], Rice Husk [21], Egg shells [22], cigarette wastes [23].

The present work uses $ZnCl_2$ as an activator agent with wasted compressed wood to predict adsorption behavior under various conditions, including isotherm and kinetic studies. Recycling damaged compressed wood to produce activated carbon represents an innovative approach that combines industrial waste management with eco-friendly water treatment solutions, providing tunable surface properties derived from the unconventional chemical composition of engineered wood.

*Corresponding Author: Email: doha.hamad2307m@coeng.uobaghdad.edu.iq

2- Materials and methods

2.1. Chemicals

$ZnCl_2$ (LOBA chemie Pvt. Ltd., India) with 99% purity, compressed wood (obtained from carpentry workshop), and CIP antibiotic (obtained from local pharmaceutical).

2.2. Activated carbon synthesis

Compressed Wood was washed with a significant amount of water to remove adhering dust, then dried at 70◦C for 48 hours to remove moisture and finally ground to the desired size. Later, activated carbon was synthesized from this compressed wood using the conventional method [24], in which the compressed wood was carbonized to 500◦C for 3 hrs. The resulting carbonized wood was impregnated with $ZnCl_2$ for 24 hr in a 1:2 ratio [25]. The impregnation sample was dried completely in a drier furnace. Lastly, to obtain the desired pH, distilled water was used to wash and dry the sample again.

The FESEM technique was applied to obtain the configuration of AC. This test using (MIRA III, Tescan Co., Czech), The functional groups were assessed by using this test in 400-4000 cm^{-1} range, using an 1800IR spectrometer instrument, Sgimadzu Co., Japan, The surface topography and roughness of AC were determined by the AFM analysis, using NaioAFM 2022, Nanosurf, Switzerland, the surface area and other related properties of AC were tests using the Brunauer Emmett Teller technique (BELSORP MINI II, BEL Co., Japan) and The Powder X-RD pattern was noted using X-Ray Diffraction instrument with a Cu-anode (PW1730 Philips Co., Netherlands).

3- Adsorption experiments

CIP antibiotic adsorption behavior variation was investigated in batch system (to provide the best control of parameters variation) with 50 mL of wastewater sample with the important and the effective parameters including time (0.25, 0.5, 1, 1.5, 2, 3…12 hr), initial CIP concentration (100, 200, 300, 400 and 500 mg/L), AC dose (0.012, 0.025, 0.05, 0.075 and 0.1 g/50 mL) in addition to temperature (20, 30, 40 and 50 C). The absorbance was measured using a UV-2900 spectrophotometer, which used a calibration curve to determine the final concentration. The elimination performance according to adsorption capacity and removal percentage was calculated using the equations [26]:

$$q_e = \frac{(C_0 - C_e) * v}{m} \quad (1)$$

$$R\% = \frac{C_0 - C_e}{C_0} * 100 \quad (2)$$

Where C_0 and C_e: CIP concentrations at initial and equilibrium time (mg/L). V: volume of sample (L). m: mass of AC (g).

4- Isotherm and kinetic models

4.1. Isotherm models

To estimate the behavior and adsorption type, isotherm models should be applied; among these models, three important models were chosen: Langmuir, Freundlich, and Temkin with their linear equations [27]:

Langmuir:

$$\frac{1}{q_e} = \frac{1}{q_m k_l C_e} + \frac{1}{q_m} \quad (3)$$

Freundlich:

$$\ln q_e = \ln k_f + \frac{1}{n} \ln C_e \quad (4)$$

Temkin:

$$q_e = B \ln A + B \mathrm{Ln} Ce \quad (5)$$

Where: C_e: Concentration of CIP at equilibrium (mg/L) qe: Adsorption capacity of CIP at equilibrium (mg/g), q_m: Maximum adsorption capacity, K_l: (L/mg), K_f: (mg/g (L/mg) $^{1/n}$): Adsorption constant of the two models, n: parameter signifies the affinity of the adsorbate to the adsorbent, A: (L/g) Constant of Temkin isotherm related to equilibrium energy, B: (J/mol) Heat of adsorption.

4.2. Adsorption kinetics

Applying kinetic models provides additional information about adsorption behavior. Pseudo first order (PFO), Pseudo second order (PSO), and Intra-particle diffusion (IPD) models were fitted with experimental data [28]:

Pseudo first order (PFO):

$$\ln(q_e - q_t) = \ln q_e - k_1 t \quad (6)$$

Pseudo-second order (PSO):

$$\frac{t}{q_t} = \frac{1}{k_2 q_e^2} + \frac{t}{q_e} \quad (7)$$

Intra-particle diffusion (IPD):

$$q_t = k_3 t^{\frac{1}{2}} + C \quad (8)$$

q_e = CIP adsorption capacity at equilibrium, q_t = adsorption capacity at time t, both in mg/g. k_1 (hr^{-1}) and k_2 (g/(mg ×hr)) are the constants of the models, K_3: constant rate of model (mg/g. $hr^{1/2}$). C: constant gives an idea about the boundary layer thickness.

5- Results and discussions

5.1. Characteristics of biosorbents

5.1.1. SEM analysis

Heterogeneity and course surface were clearly observed on the surface of AC with mesoparticle size, which was

irregular and ranged from 171 to 882 nm, while the pores were crack-shaped. Fig. 1 shows the AC images.

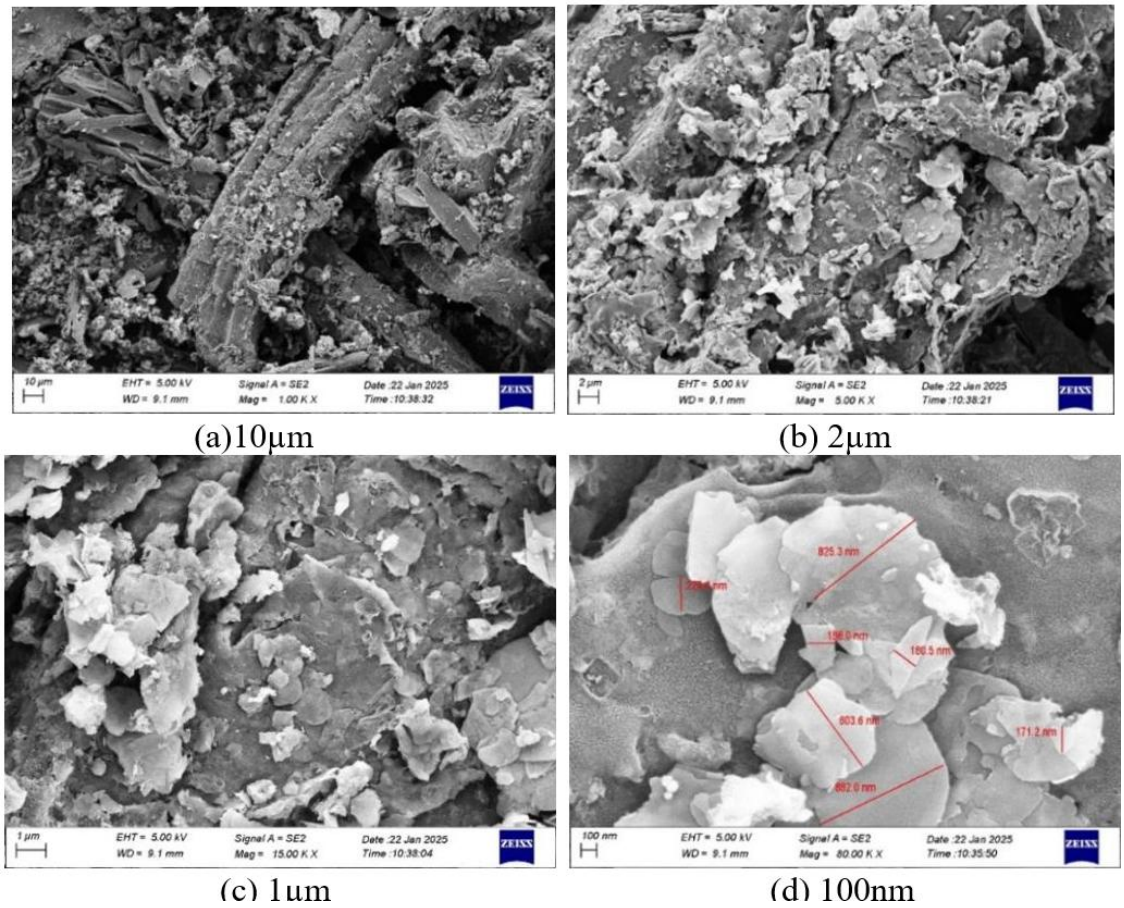

Fig. 1. SEM images

5.1.2. N_2 adsorption-desorption isotherm

Fig. 2 shows a slight curvature with efficient adsorption-desorption behavior [29]. Which matches IV isotherms, but the hysteresis loops refer to H_3 type, which is distinct from slit-like pores (seen in SEM test). This type is possibly due to monolayer behavior [30]. Surface Area, total pore volume, and average pore diameter for AC were inserted in Table 1.

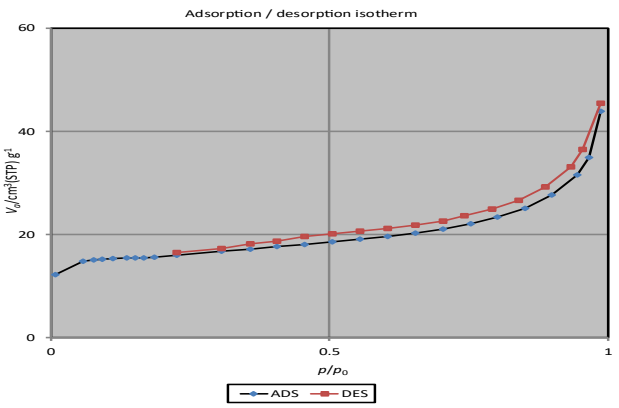

Fig. 2. N_2 adsorption-desorption isotherm

Table 1. Surface area, total pore volume, and average pore diameter for AC

S_{BET} (m^2/g)	V_{total} (cm^3/g)	Average pore diameter (nm)
518.28	0.568	3.66

5.1.3. FT-IR analysis

Fig. 3 shows the signal of 1120.64 cm^{-1} belonging to OH bending modes in the carboxylic group and the C–O vibrations [31], the peaks (605, 665.65, 665.44, 707.88, 750.31, and 788.89) cm-1 attributed to the C–H band (aromatic ring) [32]. While signal 2918.3 cm^{-1} came from a symmetric C–H vibration, which indicated the presence of an aliphatic hydrocarbon [33], the signal appeared at 2852.72 cm^{-1} corresponding to the methyl C-H band [34].

O–H bending associated with the peak of 3429.43 [12]. The spectral 1502.55 cm^{-1} can correspond to CH_3, $–CH_2–$, and C–H functional groups, in addition to the C–C band of polyphenolic aromatic rings, which refers to cellulose, hemicellulose, and lignin. Instead, this region reflects O–H vibrations, which are attributed to cellulose. It also includes contributions from C–O stretching, which refers to carboxylic groups, as well as ester, ether, and phenolic groups [35].

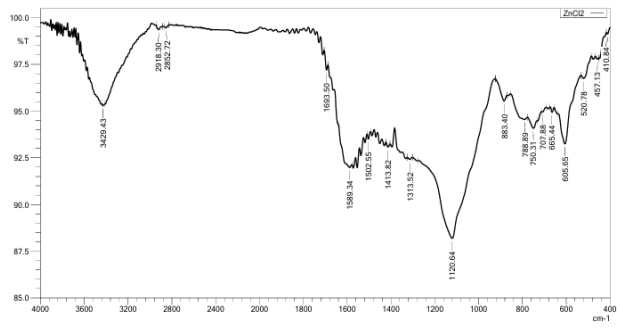

Fig. 3. FT-IR spectra

5.1.4. AFM

According to Fig. 4a, the sample of $ZnCl_2$ Activator Agent shows more uniformity compared to $ZnCl_2$ Activator Agent studied in our previous work [36]. That refers to less heterogeneity, the highest peaks around 320 nm. Fig. 4b, exposes the histogram of $ZnCl_2$ activator agent, which also refers to sized particles with mean diameters of 73.52 nm.

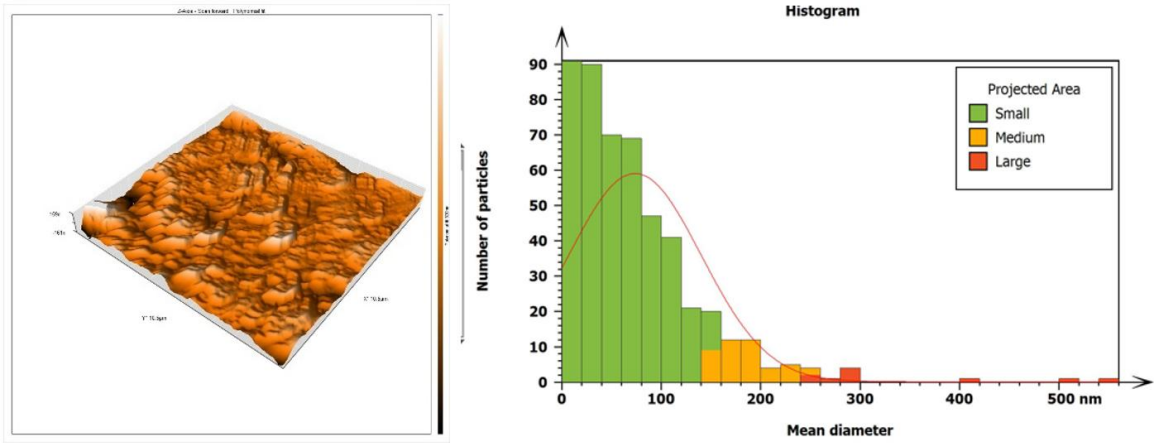

(a) (b)

Fig. 4. AFM test (a) 3D image (b) Histogram of particle size distribution

5.1.5. XRD analysis

X-Ray diffraction test notably two broadest peaks as shown in Fig. 5 2θ=32.67 contributed to ZnO generated from $ZnCl_2$ [37], while the broad band refers to amorphous structure [38] resembles to most synthesis activated carbon the second peak 2θ=58.76 which may also correspond to ZnO [37].

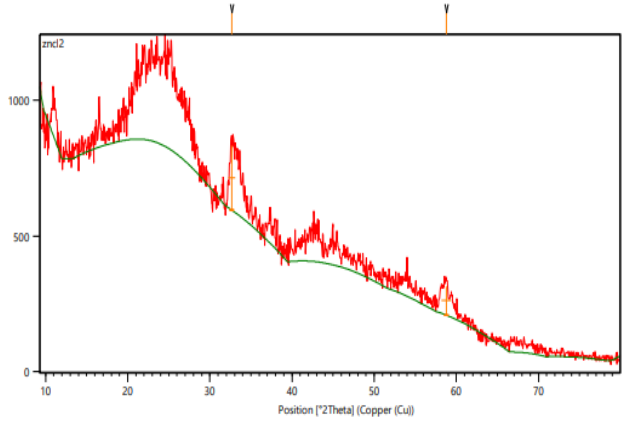

Fig. 5. XRD pattern

5.2. Adsorption performances

5.2.1. Effect of contact time and adsorption kinetics

The adsorption capacity increased steadily before reaching equilibrium within 5 hr. Pseudo-first order (PFO) and pseudo-second order (PSO) kinetic models were investigated to assess the adsorption behavior of ciprofloxacin (CIP) onto AC, based on experimental adsorption information. The modeling outcomes showed that both kinetic models provide suitable fits, as indicated by the correlation coefficients (R^2) in Fig. 6. However, the PSO model offers better agreement between the calculated and experimental data, as shown in Table 2, indicating a better description of the system, which agrees with [39].

The Intraparticle diffusion model (IPD), which yields a linear plot crossing through the origin, suggests that intraparticle diffusion controls the rate of the adsorption process. This attitude was noticed when a large amount of adsorbent was applied or when contaminant concentrations were small [40]. On the other hand, at high contaminant concentrations, the plots showed multiple steps (the line didn't pass through the origin), suggesting that the adsorption process involves several kinetic steps: external diffusion, intraparticle diffusion, and, finally, adsorption on internal wall pores [12].

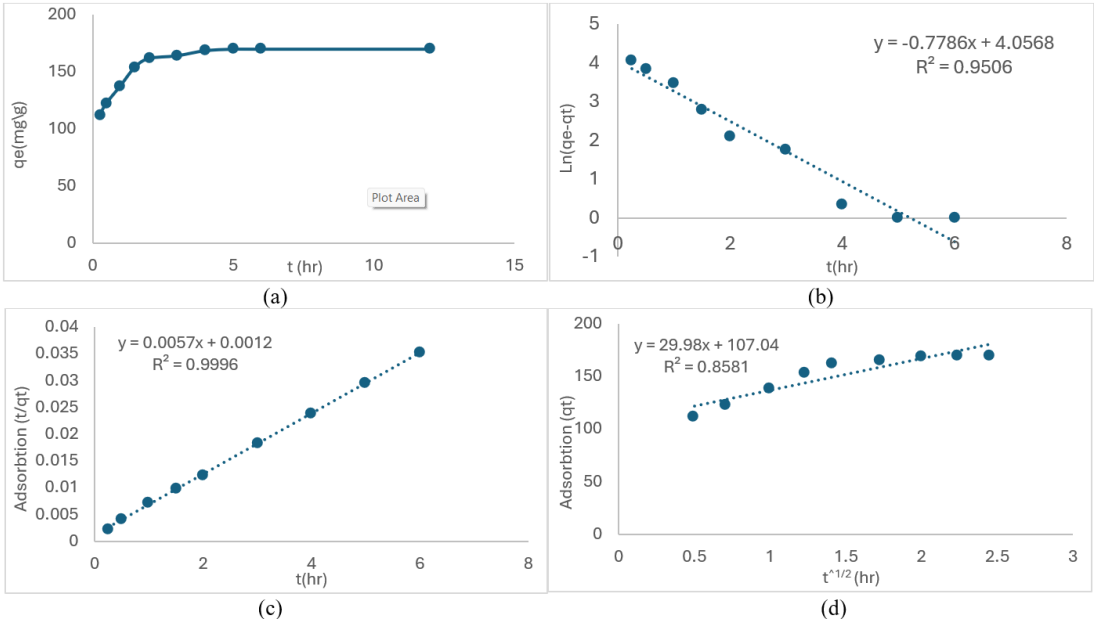

Fig. 6. (a) Time effect (b) Pseudo-first order (c) Pseudo-second order (d) Intraparticle diffusion models

Table 2. Kinetic karameters for CIP on AC with initial concentration =200 ppm at ambient temperature

Pseudo-first order model			
qe,exp(mg/g)	qe,cal(mg/g)	K_1(1/h)	R^2
170	57.39	0.77	0.95
Pseudo-second order model			
qe,exp(mg/g)	qe,cal(mg/g)	K_2(g/mg.hr)	R^2
170	200	0.02	0.99
Intra-Particle diffusion model			
qe,exp(mg/g)	C(mg/g)	K_3(mg/g hr $^{1/2}$)	R^2
170	107	29.98	0.85

5.2.2. Effect of concentration and isotherm models application

According to experimental data, the adsorption behavior of CIP at different initial concentrations was studied as shown in Fig. 7. The removal percentage was inversely affected by initial concentration, which is due to the large available number of active sites in lower concentrations.

The adsorption approach was analyzed by confirming the experimental data with three diverse isotherm models: Langmuir, Temkin, and Freundlich. The correlation coefficient (R^2) for the models was used to assess which model best fits the experimental data.

The Langmuir isotherm assumes that adsorption occurs on a homogeneous surface, forming a monolayer. The maximum adsorption capacity was attained when the adsorbate completely covered the adsorbent surface [41], yielding 454 mg/g. According to this model, with an R^2 value of 0.99. The equilibrium parameter (RL) ranged from 0 to 1, indicating that the process was favorable [42].

In the Freundlich model, $1/n < 1$ indicates that the adsorption process is favorable, simple, and physical in nature [43]. while the Freundlich constant (K_F) rises with the increase in temperature, demonstrating strong attraction between AC and CIP molecules [15]. The Freundlich model correlation factor ($R^2 = 0.995$) was the highest, indicating the best-fitting behavior; this result agrees with [26]. Applying the Root Mean Square error (RMSE) [44] yields the minimum value for the Langmuir model, indicating the best fit of the experimental data to this model.

The Temkin model clearly adapts the adsorbate-adsorbent surface interactions. Its essential hypotheses include:

(i) The adsorption heat declines linearly during coverage of the adsorbent surface with progressive adsorption and linearly with increasing surface coverage.

(ii) The attraction energies are distributed uniformly until they reach the maximum energy of binding.

Moreover, the Temkin equation assumes that the reduction in adsorption heat follows a logarithmic pattern [41]. The relative parameters for these models are presented in Table 3, where the Temkin model yields a lower R2 (0.91).

5.2.5. Effects of temperature and thermodynamic analysis

The adsorption capacity and removal efficiency of CIP decreased with increasing temperature, indicating an exothermic adsorption process. Relative parameters were assessed by incubating at temperatures ranging from 293 K to 323 K (Fig. 8) with an initial CIP concentration of 200 mg/L, while maintaining the other parameters at fixed conditions. Table 4 presents the calculated parameters. A spontaneous process was inferred from negative $\Delta G°$ values, indicating thermodynamic favorability.

Negative $\Delta H°$ indicates an exothermic process; these results agree with [45, 12], which is attributed to the active sites' lower temperature being less than the energy released during adsorption. In contrast, when the active site-dependent temperature exceeds the energy required by the CIP-AC interaction, the process is endothermic [46]. The negative value of entropy is revealed to decrease in disorder.

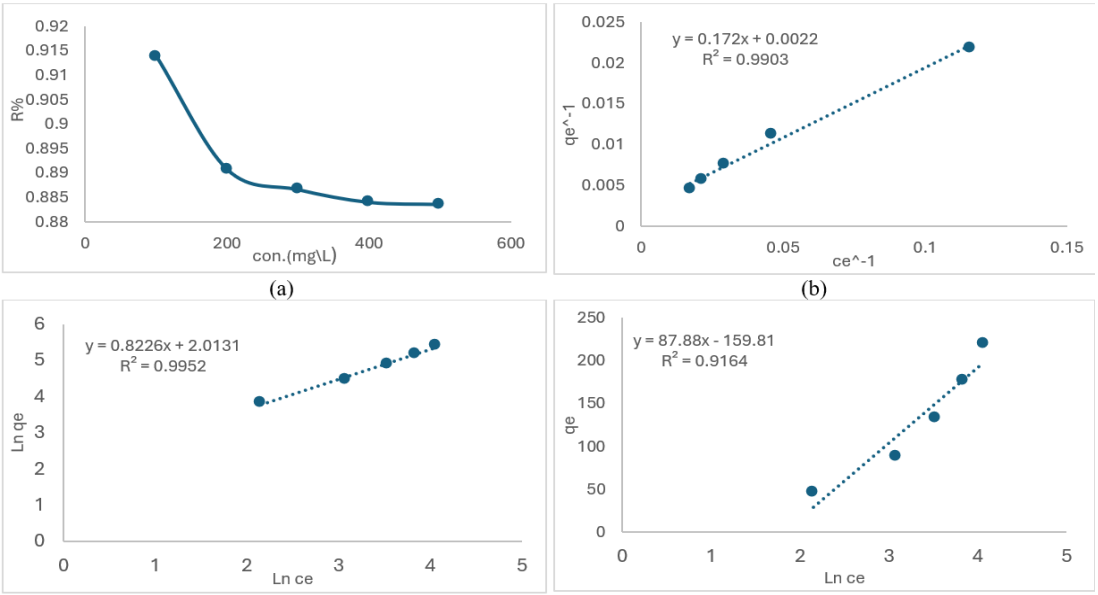

Fig. 7. (a) Concentration effect (b) Langmuir (c) Freundlich (d) Temkin models

Table 3. Isotherm parameters for CIP adsorption on AC at ambient temperature

Isotherm	Langmuir			Freundlich			Temkin		
Parameters	q_m	K_L	R^2	K_F	n	R^2	A	B	R^2
CIP	454	0.012	0.99	7.5	1.2	0.995	0.16	87.88	0.91

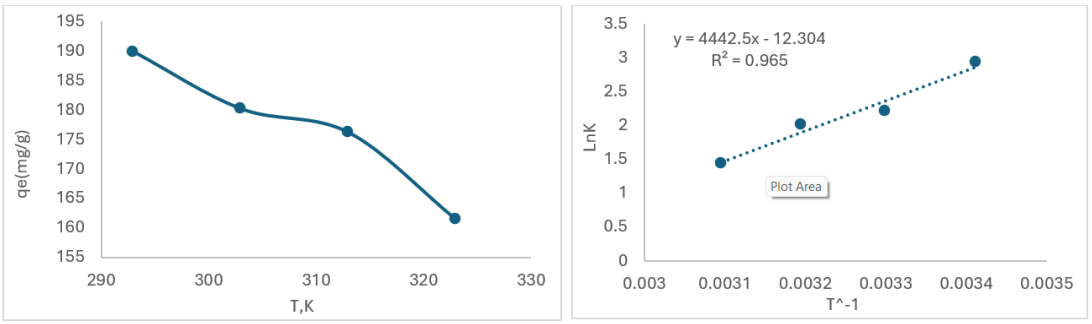

Fig. 8. (a) Temperature effect (b) thermodynamic analysis

Table 4. Thermodynamic parameters

T, K	ΔG, J/mol	ΔH, J/mol	ΔS, J/mol.K
293	-7120.09		
303	-5553.37	-534.33	-1.47
313	-5199.68		
323	-3838.41		

5.2.4. Effect of AC dosage

The effect of the CIP removal was assessed within a range of 0.012, 0.025, 0.05, 0.075, 0.1 g/50 mL aqueous solution, according to efficiency (%) and adsorption capacity (mg/g), which is shown in Fig. 9, illustrating an inverse effect on the removal efficiency and adsorption capacity.

The increase in removal efficiency can be attributed to the excess of vacant active binding sites, achieved by increasing the dosage of activated carbon (AC). Nevertheless, extreme increases in the AC dosage didn't lead to a notable increase in removal efficiency, because the driving force decreased at low CIP concentrations despite the available active sites.

The little amount of AC dosage achieved elevated adsorption capacity (471 mg/g), while the highest removal efficiency (0.95) was obtained in a larger adsorbent dosage.

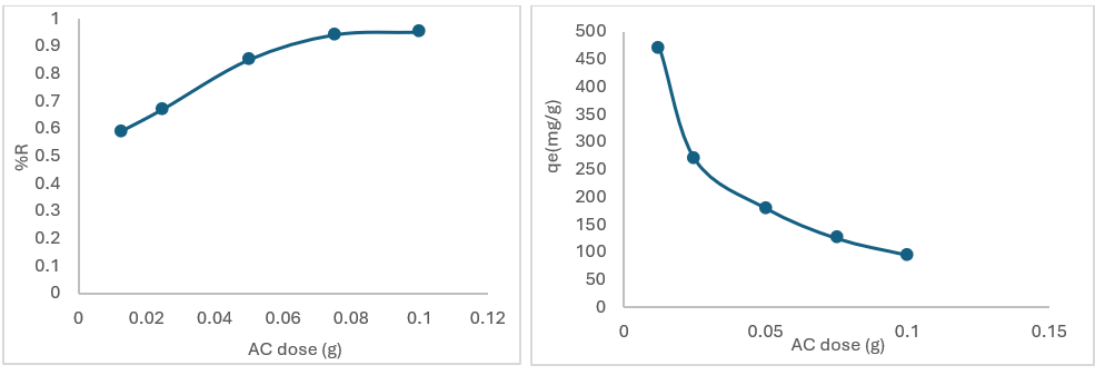

(a) (b)

Fig. 9. (a) AC dose effect with R% (b) AC dose effect with adsorption capacity

5.2.5. Effect of PH

The surface charge of the adsorbent and adsorbate is affected by pH changes, making it an essential factor to study [47]. According to many studies, the optimal pH for CIP removal ranged from 6 to 8.5 [48], which is attributed to the zwitterionic charge of the CIP surface in this pH range [49]. Therefore, pH has a slight effect on CIP adsorption, which agrees with [34]. The adsorption capacity of compressed wood precursors was compared with other precursors reported in previous studies (Table 5).

Table 5. Comparison of different precursors on CIP adsorption

Precursor	Maximum Adsorption,mg/g	Reference
Kiwi peels	40	[50]
Sterculia villosa Roxb shells	81.97	[51]
Prosopis juliflora	250	[46]
Cassia bakeriana seed pods	600	[52]
Compressed wood	220	Current study
Peony seeds shell	782	[34]

6- Adsorption mechanism

The possible adsorption mechanism of CIP on AC can be discussed based on results from spectroscopic tests, isotherms, kinetics, and thermodynamic analyses. FTIR spectra showed that the sample contained oxygen groups such as O-H, C-O-C, and C=O, which facilitated adsorption by enabling molecular interactions between CIP and AC [53]. The π-π interaction could be a significant mechanism due to the aromatic ring in the CIP structure [54]; moreover, the low solubility of CIP, which tends to hydrophobic interaction [50].

The nature charge of CIP is neutral through the range PH (6.1 to 8.7), indicating that no significant electrostatic interactions occur. Bulk diffusion also plays a good role, especially at high concentrations. Also, hydrogen bonds form due to the presence of hydroxyl and carboxyl groups [53]. ΔG^0 values less than 20KJ/mol indicate physisorption behavior, while the desorption effectiveness of acids or bases corresponds to the chemisorption mechanism [50].

In summary, this adsorption process involves multiple mechanisms, including π-π interactions, hydrophobic interactions, bulk diffusion, and hydrogen bonding, in addition to physical and chemical adsorption.

7- Recycling of activated carbon

Standard recovery techniques using chemical agents (acidic or alkaline) may produce secondary pollutants, whereas the pyrolysis method [34] shows better results. This procedure accomplished by heating the used AC according to the exact condition of the initial synthesis of AC for one hour. pyrolysis recoverability gives a good result after three cycles (qe = 101.08 mg/g compared to 170.13 mg/g by first cycle) as shown in Fig. 10. Which was less than our previous study [36], that deals with KOH as activating agent. This is attributed to the presence of metastable multilayers in adsorption via KOH as an activating agent, AC.

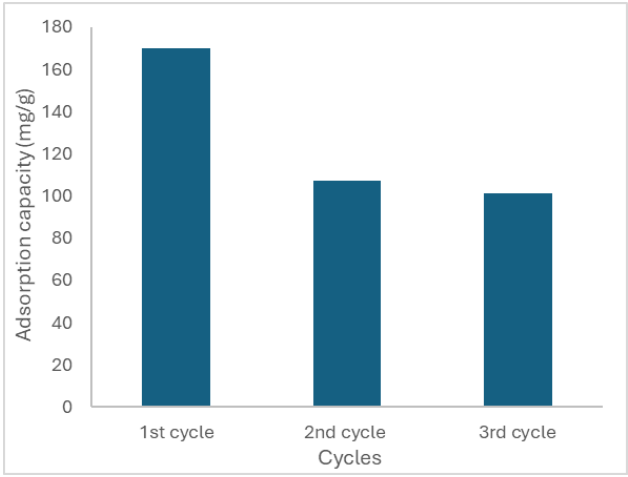

Fig. 10. Adsorption of CIP by AC after 3 cycles

8- Conclusion

This study aimed to upgrade compressed wood waste into an adsorbent (activated carbon) for the elimination of emerging pollutants from wastewater. The adsorbent was characterized using various analytical methods (SEM, BET, FTIR, AFM, and XRD), which provided

information on the properties of the compressed wood AC.

Simulated wastewater with ciprofloxacin was used to study and assess the performance of the synthesized compressed wood AC according to removal percentage R% (91%) and adsorption capacity mg/g (220 mg/g). At the same time, q_{max} was 454 mg/g. In addition to applying models of isotherm and kinetic, which were good matches with the Freundlich and Pseudo-second order. The thermodynamic analysis indicates a spontaneous adsorption process and exothermic behavior ($\Delta G^{\circ} < 0$, $\Delta H^{\bullet} = -534$, $\Delta S^{\bullet} = -1.47$). To enable regeneration of the adsorbent, pyrolysis recovery shows good results after three cycles.

References

[1] V. Rizzi et al., "Commercial bentonite clay as low-cost and recyclable 'natural' adsorbent for the Carbendazim removal/recover from water: Overview on the adsorption process and preliminary photodegradation considerations," *Colloids and Surfaces A: Physicochemical and Engineering Aspects*, vol. 602, p. 125060, Oct. 2020, https://doi.org/10.1016/j.colsurfa.2020.125060

[2] G. Enaime, A. Baçaoui, A. Yaacoubi, and M. Lübken, "Biochar for wastewater treatment-conversion technologies and applications," *In Applied Sciences (Switzerland)*, May 01, 2020, MDPI AG. https://doi.org/10.3390/app10103492

[3] Z. Chen et al., "Photocatalytic antifouling properties of novel PVDF membranes improved by incorporation of SnO2-GO nanocomposite for water treatment," *Separation and Purification Technology*, vol. 259, p. 118184, Mar. 2021, https://doi.org/10.1016/j.seppur.2020.118184

[4] A. E. Abdelhamid, A. E. Elsayed, M. Naguib, and E. A. Ali, "Effective Dye Removal by Acrylic-Based Membrane Constructed from Textile Fibers Waste," *Fibers and Polymers*, vol. 24, no. 7, pp. 2391–2399, Jul. 2023, https://doi.org/10.1007/s12221-023-00247-z

[5] T. Thiebault, "Sulfamethoxazole/Trimethoprim ratio as a new marker in raw wastewaters: A critical review," *Science of The Total Environment*, vol. 715, p. 136916, May 2020, https://doi.org/10.1016/j.scitotenv.2020.136916

[6] S. D. Martinho, V. C. Fernandes, S. A. Figueiredo, and C. Delerue-Matos, "Microplastic Pollution Focused on Sources, Distribution, Contaminant Interactions, Analytical Methods, and Wastewater Removal Strategies: A Review," *International Journal of Environmental Research and Public Health*, vol. 19, no. 9, p. 5610, May 2022, https://doi.org/10.3390/ijerph19095610

[7] E. Brillas, "Progress of homogeneous and heterogeneous electro-Fenton treatments of antibiotics in synthetic and real wastewaters. A critical review on the period 2017–2021," *Science of The Total Environment*, vol. 819, p. 153102, May 2022, https://doi.org/10.1016/j.scitotenv.2022.153102

[8] O. Falyouna, M. Faizul Idham, I. Maamoun, K. Bensaida, Y. Sugihara, and O. Eljamal, "Promotion of ciprofloxacin adsorption from contaminated solutions by oxalate modified nanoscale zerovalent iron particles 2," *Journal of Molecular Liquids*, Vol. 359, p. 1193231 August 2022, https://doi.org/10.1016/j.molliq.2022.119323

[9] E. Brillas and J. M. Peralta-Hernández, "Antibiotic removal from synthetic and real aqueous matrices by peroxymonosulfate-based advanced oxidation processes. A review of recent development," *Chemosphere*, Mar. 01, 2024, Elsevier Ltd. https://doi.org/10.1016/j.chemosphere.2024.141153

[10] H. Fan, Y. Ma, J. Wan, Y. Wang, Z. Li, and Y. Chen, "Adsorption properties and mechanisms of novel biomaterials from banyan aerial roots via simple modification for ciprofloxacin removal," *Science of The Total Environment*, vol. 708, p. 134630, Mar. 2020, https://doi.org/10.1016/j.scitotenv.2019.134630

[11] O. Falyouna, I. Maamoun, K. Bensaida, A. Tahara, Y. Sugihara, O. Eljamal, "Encapsulation of iron nanoparticles with magnesium hydroxide shell for remarkable removal of ciprofloxacin from contaminated water," *Journal of colloid and Interface science*, vol. 605, pp. 813–827, Jan. 2022, https://doi.org/10.1016/j.jcis.2021.07.154

[12] N. Sharifpour, F. M. Moghaddam, G. Mardani, and M. Malakootian, "Evaluation of the activated carbon coated with multiwalled carbon nanotubes in removal of ciprofloxacin from aqueous solutions," *Applied Water Science*, vol. 10, no. 6, Jun. 2020, https://doi.org/10.1007/s13201-020-01229-9

[13] D. Yang et al., "Biochar-supported nanoscale zero-valent iron can simultaneously decrease cadmium and arsenic uptake by rice grains in co-contaminated soil," *Science of The Total Environment*, vol. 814, p. 152798, Mar. 2022, https://doi.org/10.1016/j.scitotenv.2021.152798

[14] N. T. Nguyen, T. H. Dao, T. T. Truong, T. M. T. Nguyen, and T. D. Pham, "Adsorption characteristic of ciprofloxacin antibiotic onto synthesized alpha alumina nanoparticles with surface modification by polyanion," *Journal of Molecular Liquids*, vol. 309, p. 113150, Jul. 2020, https://doi.org/10.1016/j.molliq.2020.113150

[15] O. S. Agboola and O. S. Bello, "Enhanced adsorption of ciprofloxacin from aqueous solutions using functionalized banana stalk," *Biomass Conversion and Biorefinery*, vol. 12, no. 12, pp. 5463–5478, Dec. 2022, https://doi.org/10.1007/s13399-020-01038-9

[16] V. J. Landin-Sandoval, D. I. Mendoza-Castillo, A. Bonilla-Petriciolet, I. A. Aguayo-Villarreal, H. E. Reynel-Avila, and H. A. Gonzalez-Ponce, "Valorization of agri-food industry wastes to prepare adsorbents for heavy metal removal from water," *Journal of Environmental Chemical Engineering*, vol. 8, no. 5, p. 104067, Oct. 2020, https://doi.org/10.1016/j.jece.2020.104067

[17] W. Widiyastuti, M. Fahrudin Rois, N. M. I. P. Suari, and H. Setyawan, "Activated carbon nanofibers derived from coconut shell charcoal for dye removal application," *Advanced Powder Technology*, vol. 31, no. 8, pp. 3267–3273, Aug. 2020, https://doi.org/10.1016/j.apt.2020.06.012

[18] R. R. Karri, J. N. Sahu, and B. C. Meikap, "Improving efficacy of Cr (VI) adsorption process on sustainable adsorbent derived from waste biomass (sugarcane bagasse) with help of ant colony optimization," *Industrial Crops and Products*, vol. 143, p. 111927, Jan. 2020, https://doi.org/10.1016/j.indcrop.2019.111927

[19] S. M. Kharrazi, N. Mirghaffari, M. M. Dastgerdi, and M. Soleimani, "A novel post-modification of powdered activated carbon prepared from lignocellulosic waste through thermal tension treatment to enhance the porosity and heavy metals adsorption," *Powder Technology*, vol. 366, pp. 358–368, Apr. 2020, https://doi.org/10.1016/j.powtec.2020.01.065

[20] Y. Oday and H. A. Al-Jendeel, "Synthesis and Characterization of Acidic Activated Carbon from Corncobs for Adsorption Desulfurization of Simulated Crude Oil," *Journal of Ecological Engineering*, vol. 25, no. 8, pp. 141–150, Aug. 2024, https://doi.org/10.12911/22998993/189895

[21] H. Abbas and A. S. Abbas, "Adsorption of Flagyl on Prepared Ash from Rice Husk," *Iraqi Journal of Chemical and Petroleum Engineering*, vol. 22, no. 4, pp. 11–17, Dec. 2021, https://doi.org/10.31699/ijcpe.2021.4.2

[22] M. Aravind and M. Amalanathan, "Structural, morphological, and optical properties of country egg shell derived activated carbon for dye removal," *Materials Today: Proceedings*, vol. 43, pp. 1491–1495, 2021, https://doi.org/10.1016/j.matpr.2020.09.311

[23] M. J. Ahmed, B. H. Hameed, and M. A. Khan, "Recent progress on carbonaceous materials-based adsorbents derived from cigarette wastes for sustainable remediation of aquatic pollutants: A review," *Journal of Analytical and Applied Pyrolysis*, vol. 183, p. 106779, Oct. 2024, https://doi.org/10.1016/j.jaap.2024.106779

[24] N. A. Raheem, N. S. Majeed, and Z. Al Timimi, "Phenol Adsorption from Simulated Wastewater Using Activated Spent Tea Leaves," *Iraqi Journal of Chemical and Petroleum Engineering*, vol. 25, no. 1, pp. 95–102, Mar. 2024, https://doi.org/10.31699/ijcpe.2024.1.9

[25] N. S. Razali et al., "High-Surface-Area-Activated Carbon Derived from Mango Peels and Seeds Wastes via Microwave-Induced ZnCl2 Activation for Adsorption of Methylene Blue Dye Molecules: Statistical Optimization and Mechanism," *Molecules*, vol. 27, no. 20, p. 6947, Oct. 2022, https://doi.org/10.3390/molecules27206947

[26] S. M. Al-Jubouri, H. A. Al-Jendeel, S. A. Rashid, and S. Al-Batty, "Antibiotics adsorption from contaminated water by composites of ZSM-5 zeolite nanocrystals coated carbon," *Journal of Water Process Engineering*, vol. 47, p. 102745, Jun. 2022, https://doi.org/10.1016/j.jwpe.2022.102745

[27] H. Aljendeel, H. Rasheed, N. Ahmedzeki, and M. Alhassani, "Dual Application of Al-Kheriat of Removal of Arsenic from Aqueous Solution and Acting as Rodenticide," *Journal of Ecological Engineering*, vol. 24, no. 4, pp. 16–26, Apr. 2023, https://doi.org/10.12911/22998993/159335

[28] K. K. Hummadi, "Optimal Operating Conditions for Adsorption of Heavy Metals from an Aqueous Solution by an Agriculture Waste," *Iraqi Journal of Chemical and Petroleum Engineering*, vol. 22, no. 2, pp. 27–35, Jun. 2021, https://doi.org/10.31699/ijcpe.2021.2.4

[29] S. B. Daffalla, H. Mukhtar, and M. S. Shaharun, "Preparation and characterization of rice husk adsorbents for phenol removal from aqueous systems," *PLoS One*, vol. 15, no. 12, p. e0243540, Dec. 2020, https://doi.org/10.1371/journal.pone.0243540

[30] G. Dragan, V. Kutarov, E. Schieferstein, and A. Iorgov, "Adsorption hysteresis in open slit-like micropores," *Molecules*, vol. 26, no. 16, Aug. 2021, https://doi.org/10.3390/molecules26165074

[31] K. Kiełbasa et al., "Carbon Dioxide Adsorption over Activated Carbons Produced from Molasses Using H2SO4, H3PO4, HCl, NaOH, and KOH as Activating Agents," *Molecules*, vol. 27, no. 21, Nov. 2022, https://doi.org/10.3390/molecules27217467

[32] Z. Sun et al., "Corncob-derived Activated Carbon for Efficient Adsorption Dye in Sewage," *ES Food and Agroforestry*, vol. 4, pp. 61–74, Jun. 2021, https://doi.org/10.30919/esfaf473

[33] S. Foorginezhad, M. M. Zerafat, M. Asadnia, and G. Rezvannasab, 'Activated porous carbon derived from sawdust for CO2 capture', *Materials Chemistry and Physics*, vol. 317, Apr. 2024, https://doi.org/10.1016/j.matchemphys.2024.129177

[34] P. Liu, T. Song, R. Deng, X. Hou, and J. Yi, "The efficient removal of congo red and ciprofloxacin by peony seeds shell activated carbon with ultra-high specific surface area," *Environmental Science and Pollution Research*, vol. 30, no. 18, pp. 53177–53190, Apr. 2023, https://doi.org/10.1007/s11356-023-26146-7

[35] Y. Gao, Q. Yue, B. Gao, and A. Li, "Insight into activated carbon from different kinds of chemical activating agents: A review," *Science of The Total Environment*, vol. 746, p. 141094, Dec. 2020, https://doi.org/10.1016/j.scitotenv.2020.141094

[36] D. H. Hamad and H. A. Al-Jendeel, "Study of ciprofloxacin adsorption using activated carbon from compressed wood: Evaluation of performance and efficiency in pollutant removal," *Journal of Ecological Engineering*, vol. 26, no. 9, pp. 440–448, Sep. 2025, https://doi.org/10.12911/22998993/205476

[37] S. Hadi, E. Taheri, M. M. Amin, A. Fatehizadeh, and E. C. Lima, "Fabrication of activated carbon from pomegranate husk by dual consecutive chemical activation for 4-chlorophenol adsorption," *Environmental Science and Pollution Research*, vol. 28, no. 11, pp. 13919–13930, Mar. 2021, https://doi.org/10.1007/s11356-020-11624-z

[38] J. Serafin, K. Kiełbasa, and B. Michalkiewicz, "The new tailored nanoporous carbons from the common polypody (Polypodium vulgare): The role of textural properties for enhanced CO2 adsorption," *Chemical Engineering Journal*, vol. 429, p. 131751, Feb. 2022, https://doi.org/10.1016/j.cej.2021.131751

[39] H. Ji, T. Wang, T. Huang, B. Lai, and W. Liu, "Adsorptive removal of ciprofloxacin with different dissociated species onto titanate nanotubes," *Journal of Cleaner Production*, vol. 278, p. 123924, Jan. 2021, https://doi.org/10.1016/j.jclepro.2020.123924

[40] M. Gayathiri, T. Pulingam, K. T. Lee, and K. Sudesh, "Activated carbon from biomass waste precursors: Factors affecting 1 production and adsorption mechanism," *Chemosphere*, Vol. 294, p. 133764, May 2022, https://doi.org/10.1016/j.chemosphere.2022.133764

[41] E. S. M. Al-Mashhadani, M. K. H. Al-Mashhadani, and M. A. Al-Maari, "Biosorption of Ciprofloxacin (CIP) using the Waste of Extraction Process of Microalgae: The Equilibrium Isotherm and Kinetic Study," *Iraqi Journal of Chemical and Petroleum Engineering*, vol. 24, no. 4, pp. 1–15, Dec. 2023, https://doi.org/10.31699/ijcpe.2023.4.1

[42] B. Tanhaei, A. Ayati, E. Iakovleva, and M. Sillanpää, "Efficient carbon interlayed magnetic chitosan adsorbent for anionic dye removal: Synthesis, characterization and adsorption study," *International Journal of Biological Macromolecules*, vol. 164, pp. 3621–3631, Dec. 2020, https://doi.org/10.1016/j.ijbiomac.2020.08.207

[43] J. O. Ighalo et al., "Mitigation of clofibric acid pollution by adsorption: A review of recent developments," *Journal of Environmental Chemical Engineering*, vol. 8, no. 5, Oct. 2020, https://doi.org/10.1016/j.jece.2020.104264

[44] T. O. Hodson, 'Root-mean-square error (RMSE) or mean absolute error (MAE): when to use them or not', *Geoscintific Model Development*, vol. 15, no. 14, pp. 5481–5487, Jul. 2022, https://doi.org/10.5194/gmd-15-5481-2022

[45] O. A. A. Eletta, I. O. Tijani, and J. O. Ighalo, "Adsorption of Pb(II) and Phenol from Wastewater Using Silver Nitrate Modified Activated Carbon from Groundnut (Arachis hypogaea L.) Shells." *The West Indian Journal of Engineering*, Vol.43, no.1, pp.26-35, July 2020.

[46] A. Chandrasekaran, C. Patra, S. Narayanasamy, and S. Subbiah, "Adsorptive removal of Ciprofloxacin and Amoxicillin from single and binary aqueous systems using acid-activated carbon from Prosopis juliflora," *Environmental Research*, vol. 188, Sep. 2020, https://doi.org/10.1016/j.envres.2020.109825

[47] D. Balarak and G. McKay, "Utilization of MWCNTs/Al 2 O 3 as adsorbent for ciprofloxacin removal: equilibrium, kinetics and thermodynamic studies," *Journal of Environmental Science and Health*, Part A, vol. 56, no. 3, pp. 324–333, Feb. 2021, https://doi.org/10.1080/10934529.2021.1873674

[48] M. Malakootian, M. Faraji, M. Malakootian, and M. Nozari, "Ciprofloxacin removal from aqueous media by adsorption process: A systematic review and meta-analysis," *Desalination and Water Treatment*, vol. 229, pp. 252–282, Jul. 2021, https://doi.org/10.5004/dwt.2021.27334

[49] C. A. Igwegbe, S. N. Oba, C. O. Aniagor, A. G. Adeniyi, and J. O. Ighalo, "Adsorption of ciprofloxacin from water: A comprehensive review," *Korean Society of Industrial Engineering Chemistry*, Jan. 25, 2021, https://doi.org/10.1016/j.jiec.2020.09.023

[50] J. Gubitosa, V. Rizzi, D. Cignolo, P. Fini, F. Fanelli, and P. Cosma, "From agricultural wastes to a resource: Kiwi Peels, as long-lasting, recyclable adsorbent, to remove emerging pollutants from water. The case of Ciprofloxacin removal," *Sustainable Chemistry and Pharmacy*, vol. 29, Oct. 2022, https://doi.org/10.1016/j.scp.2022.100749

[51] A. Kumar, C. Patra, S. Kumar, and S. Narayanasamy, "Effect of magnetization on the adsorptive removal of an emerging contaminant ciprofloxacin by magnetic acid activated carbon," *Environmental Research*, vol. 206, p. 112604, Apr. 2022, https://doi.org/10.1016/j.envres.2021.112604

[52] N. Theamwong et al., "Activated carbons from waste Cassia bakeriana seed pods as high-performance adsorbents for toxic anionic dye and ciprofloxacin antibiotic remediation," *Bioresource Technology*, vol. 341, p. 125832, Dec. 2021, https://doi.org/10.1016/j.biortech.2021.125832

[53] S. Dou, X.-X. Ke, Z.-D. Shao, L.-B. Zhong, Q.-B. Zhao, and Y.-M. Zheng, "Fish scale-based biochar with defined pore size and ultrahigh specific surface area for highly efficient adsorption of ciprofloxacin," *Chemosphere*, vol. 287, p. 131962, Jan. 2022, https://doi.org/10.1016/j.chemosphere.2021.131962

[54] J. K. Bediako et al., "Evaluation of orange peel-derived activated carbons for treatment of dye-contaminated wastewater tailings," *Environmental Science and Pollution Research*, vol. 27, no. 1, pp. 1053–1068, Jan. 2020, https://doi.org/10.1007/s11356-019-07031-8

امتصاص السيبروفلوكساسين عبر الكربون النشط للخشب المضغوط مع عامل تنشيط $ZnCl_2$ من مياه الصرف الصحي المحاكاة: دراسة الآلية

ضحى حميد حمد [١،*]، حيدر عبد الكريم الجنديل [١]، مصطفى محمد هذال [٢]

١ قسم الهندسة الكيمياوية، كلية الهندسة، جامعة بغداد، العراق
٢ مختبر بحوث الحلول المستدامة، جامعة بانونيا، فيسبريم، المجر

الخلاصة

تهدف الدراسة الحالية إلى تصنيع الكربون المنشط (AC) عبر الخشب المضغوط باستخدام عامل منشط $ZnCl_2$، وتقييم كفاءة إزالة السيبروفلوكساسين (CIP) من مياه الصرف الصحي المحاكاة. تم تشخيص الكربون المنشط الناتج بتقنيات متعددة، مثل المجهر الإلكتروني الماسح (SEM)، وفحص سلوك الامتزاز (BET)، ومطياف الأشعة تحت الحمراء (FTIR)، ومجهر القوة الذرية (AFM)، وتقنية حيود الأشعة السينية (XRD). تؤكد نتائج الامتزاز على أداء امتزاز عالٍ، حيث يزيل ٩١٪ من (CIP) خلال ٥ ساعات، عند تركيز أولي ١٠٠ ملغم/لتر من الملوث، وجرعة كربون منشط مقدارها ٢ غ/لتر. تتوافق البيانات التجريبية مع نموذج معادلة فروندليش (R^2 =٠.٩٩٥) ولانكمويز بنسبة تطابق منافسة بينما اظهرت معادلة الجذر التربيعي لمتوسط مربعات الاخطاء تطابق اعلى مع نموذج لانكمويز، بالإضافة إلى نموذج لانغمويز بمعامل تطابق تنافسي (R^2=٠,٩٩)، الذي يشير إلى خاصية الامتزاز متعدد الطبقات وسطح غير المتجانس. علاوة على ذلك، وصفت البيانات الحركية بنسبة تطابق (R^2 = 0.999) مع نموذج الدرجة شبه الثانية. تشير الديناميكية الحرارية للامتصاص إلى امتزاز تلقائي ذي سلوك طارد للحرارة (ΔG°<٠، ΔH°<٠، ΔS°<٠). يساهم مزيج من الآليات في عملية الامتزاز مثل تفاعل π-π، التفاعل الطارد للماء، انتشار الكتلة، الروابط هيدروجينية)، بالإضافة إلى آليات الامتزاز الفيزيائية والكيميائية. تُعطي قابلية الاسترداد بالتحلل الحراري نتيجة جيدة بعد ثلاث دورات (ملغ/غم qe=١٠١.٠٨ مقارنة بـ ١٧٠.١٣ ملغ/ غم في الدورة الأولى).

الكلمات الدالة: الخشب المضغوط، الكاربون المنشط، عامل التنشيط $ZnCl_2$، الانتشار داخل الجسيمات، نموذج تمكن، سيبروفلوكساسين، الية الامتزاز، الامتزاز الباعث للحرارة.